Electronic Supplementary Information for 'Molecular insights on Poly(N-isopropylacrylamide) coil-to-globule transition induced by pressure'

Letizia Tavagnacco,[1] Ester Chiessi,[2] and Emanuela Zaccarelli[1]

[1] *CNR-ISC and Department of Physics, Sapienza University of Rome, Piazzale A. Moro 2, 00185, Rome, Italy.*

[2] *Department of Chemical Sciences and Technologies, University of Rome Tor Vergata, Via della Ricerca Scientifica I, 00133 Rome, Italy.**

I. MODEL AND SIMULATION PROCEDURE

We investigate the pressure-temperature phase diagram of a PNIPAM linear chain in water in dilute regime. The degree of polymerization is chosen to be 30 on the basis of experimental results which showed that the solution behavior at atmospheric pressure of an oligomer made of 28 repeating units corresponds to that observed at higher degrees of polymerization [S1, S2]. Amide groups are represented with a trans geometry. PNIPAM and water are described with the OPLS-AA force field [S5] with the modifications of Siu et al. [S6] and the Tip4p/ICE [S7] model, respectively.

First, the polymer chain with an energy optimized conformation [S3, S8] was centered in a cubic box of 8.5 nm side and oriented along a box diagonal to maximize the distance between periodic images. Then, 22849 water molecules were added and an energy minimization with tolerance of 1000 $kJmol^{-1}nm^{-1}$ was carried out. The resulting system was used as initial configuration for the simulations at seven different pressure conditions, specifically 0.1 MPa, 30 MPa, 50 MPa, 100 MPa, 200 MPa, 350 MPa, and 500 MPa, in a range of temperature between 283 K and 308 K.Trajectory acquisition and analysis were carried out with the GROMACS software package (version 5.1.4) [S9, S10]. The molecular viewer software package VMD was used for graphic visualization [S11]. MD simulations were carried out in the NPT ensemble for 300 ns for each point in the P-T phase diagram. Trajectories were acquired with the leapfrog integration algorithm [S12] with a time step of 2 fs. Cubic periodic boundary conditions and minimum image convention were applied. The length of bonds involving H atoms was constrained by the LINCS procedure [S13]. The velocity rescaling thermostat coupling algorithm, with a time constant of 0.1 ps was used to control temperature [S14]. Pressure of was maintained by the Berendsen barostat [S15] using a time constant of 0.5 ps with a standard error on pressure values lower than 10%. The cutoff of nonbonded interactions was set to 1 nm and electrostatic interactions were calculated by the smooth particle-mesh Ewald method [S16]. Typically, the final 100 ns of trajectory were considered for analysis, sampling 1 frame every 5 ps.

II. TRAJECTORY ANALYSIS

The occurrence of the coil-to globule transition was monitored by calculating the radius of gyration (R_G) and the solvent accessible surface area (SASA). R_G was calculated through the equation:

$$R_g = \sqrt{\frac{\sum_i \|r_i\|^2 m_i}{\sum_i m_i}} \tag{S1}$$

where m_i is the mass of the i^{th} atom and r_i the position of the i^{th} atom with respect to the center of mass of the polymer chain. The SASA is defined as the surface of closest approach of solvent molecules to a solute molecule, where both solute and solvent are described as hard spheres. It is calculated as the van der Waals envelope of the solute molecule extended by the radius of the solvent sphere about each solute atom centre [S17]. We used a spherical probe with radius of 0.14 nm and the values of Van der Waals radii of the work of Bondi [S18, S19]. The distributions of SASA values were calculated with a bin of 0.1 nm^2. Averages were performed over the last 100 ns of trajectory.

The transition temperature (T_c) values are calculated as the average of the T_c obtained from the sigmoidal fit of the temperature dependence of R_G and SASA. Globular states are assigned to conformations with an average radius of gyration smaller than 1.2 nm.

Hydrogen bonds were evaluated adopting the geometric criteria of an acceptor-donor distance ($A \cdots D$) lower than 0.35 nm and an angle θ ($A \cdots D - H$) lower than 30°, irrespective of the AD pair. The dynamical behavior of hydrogen bonding interactions was characterized by calculating the normalized intermittent time autocorrelation function which is irrespective of intervening interruptions. The corresponding lifetime was defined as the time at which the autocorrelation function is decayed of the 50% of its amplitude to reduce statistical noise.

Hydration properties were investigated as a function of pressure and temperature. The ensemble of water molecules in the first solvation shell was sampled by selecting molecules having the water oxygen atom at a distance from PNIPAM nitrogen/oxygen atoms lower than 0.35 nm (hydrophilic water molecules) or a distance from methyl carbon atoms of PNIPAM lower than 0.55 nm (hydrophobic water molecules). Hydrogen bonding between water molecules of the first solvation shell was also analysed. The clustering of water molecules belonging to the first solvation shell was analysed by calculating the population of clusters formed by hydrogen bonded molecules.

The local water structuring was characterized by calculating the tetrahedrality order parameter q for hydration and bulk water molecules. q is defined as:

$$q \;=\; 1 - \frac{3}{8}\sum_{j=1}^{3}\sum_{k=j+1}^{4}\left(\cos\psi_{jk} + \frac{1}{3}\right)^2 \tag{S2}$$

where ψ_{jk} is the angle formed by the lines joining the oxygen atom of a molecule and those of its nearest neighbours j and k. The average value of q varies between 0 (in an ideal gas) and 1 (in a perfect tetrahedral network) [S20]. In the calculation of q for hydration water molecules PNIPAM oxygen and nitrogen atoms were also taken into account.

III. COMPARISON BETWEEN TWO REPLICAS AT ATMOSPHERIC PRESSURE

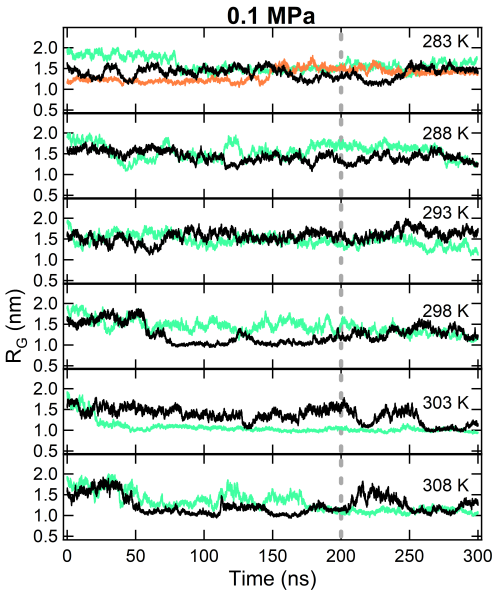

FIG. S1: Radius of gyration as a function of time at P=0.1 MPa and for T=283, 288, 293, 298, 303 and 308 K. Results of the replica 1 (first realization) and 2 (new realization) are shown in green and black, respectively. An additional simulation at 283 K starting from a globule chain conformation is displayed in orange. The vertical line marks the trajectory interval used for the analysis.

To test the reproducibility of single trajectory data, we have performed a second replica of the full temperature range at atmospheric pressure starting from a different coil conformation of the chain, which complements our first set of results for a single replica that was reported in Ref. [S4]. In addition, we further compared simulations performed at T=283K using three different initial conformations of the chain, in the extended, intermediate and collapsed state, respectively. The results of these additional simulations (replica 2) are summarized in Figures S1 and S2. Remarkably, we observe that simulations carried out at T=283K with different initial conditions, even with a starting collapsed

conformation, lead to comparable average properties of the polymer chain. Furthermore, we confirm the occurrence of the coil-to-globule transition at a similar T_c for both replicas. Importantly, the distributions of radius of gyration, displayed in Figure S3, clearly highlight the presence of multiple rearranging events of the chain conformation which signal an adequate sampling of the phase space on the chosen time interval for all studied state points. Similar findings are obtained by analyzing a different observable such as the solvent accessible surface area which is reported in Figure S4. These results confirm the robustness of our initial approach because a good reproducibility of the data is observed, even when different initial configurations are employed.

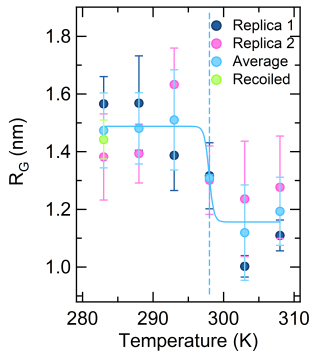

FIG. S2: Temperature dependence of PNIPAM radius of gyration. Data represent time averaged values over the last 100 ns and standard deviation for the simulations collected at pressure value of 0.1 MPa in the Replica 1 (blue), Replica 2 (pink) and average of the two replicas (light blue). Results obtained at 283 K from an initial collapsed conformation are also displayed in green. The solid line is the sigmoidal fit to the averaged data.

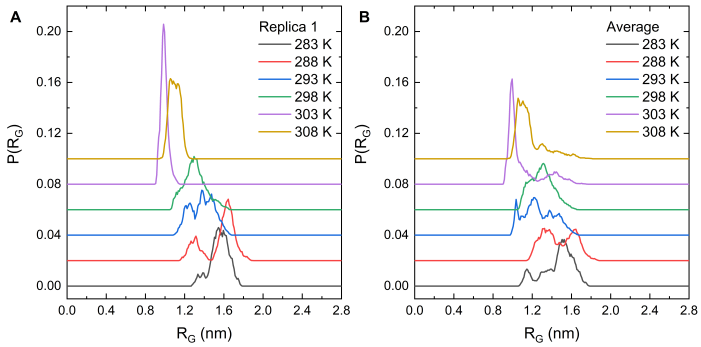

FIG. S3: Distribution of radius of gyration $P(R_G)$ at P=0.1 MPa and for T=283, 288, 293, 298, 303 and 308 K over the last 100 ns of simulation for (A) replica 1 and (B) the average of replica 1 and 2.

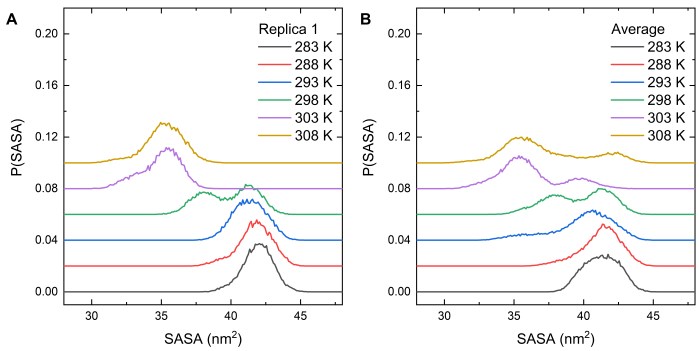

FIG. S4: Distribution of solvent accessible surface area $P(SASA)$ at P=0.1 MPa and for T=283, 288, 293, 298, 303 and 308 K over the last 100 ns of simulation for (A) replica 1 and (B) the average of replica 1 and 2.

IV. STRUCTURAL CHARACTERIZATION OF PNIPAM COIL-TO-GLOBULE TRANSITION

To identify the transition temperature T_c, we calculated the radius of gyration of the polymer chain in the last 100 ns of equilibrated run. Figure S5 shows the time evolution of the radius of gyration of the chain in the whole trajectory for the simulations of Replica 1 in the high pressure regime.

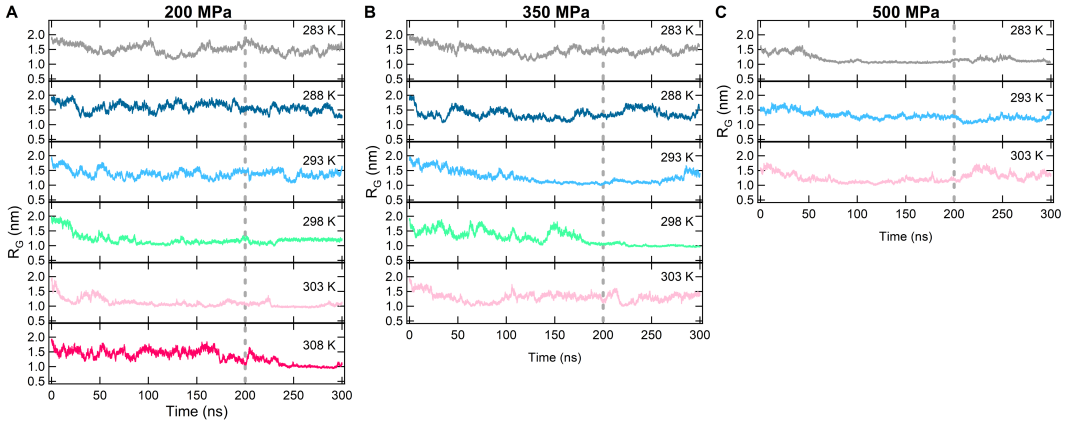

FIG. S5: Time evolution of PNIPAM radius of gyration for Replica 1 as a function of temperature at the investigated pressure values of 200 MPa (**A**), 350 MPa (**B**), and 500 MPa (**C**). Simulation results obtained at 283 K, 288 K, 293 K, 298 K, 303 K, and 308 K are displayed in grey, blue, light blue, green, pink, and red, respectively. The last 100 ns of trajectory data, marked by dashed vertical lines, were used for data analysis.

V. PNIPAM-PNIPAM HYDROGEN BONDING

The change with temperature and pressure of intrachain interactions was also monitored as a function of the topological distance between PNIPAM repeating units. Figure S6 compares the average number of hydrogen bonds between PNIPAM amide groups separated by less than 4 residues to the average number of hydrogen bonds formed between amide groups separated by more than 3 residues. The major contribution to the increase of the total number of PNIPAM-PNIPAM hydrogen bonds across the transition temperature can be ascribed to the formation of interactions between distant residues. This effect is reduced by applying pressure.

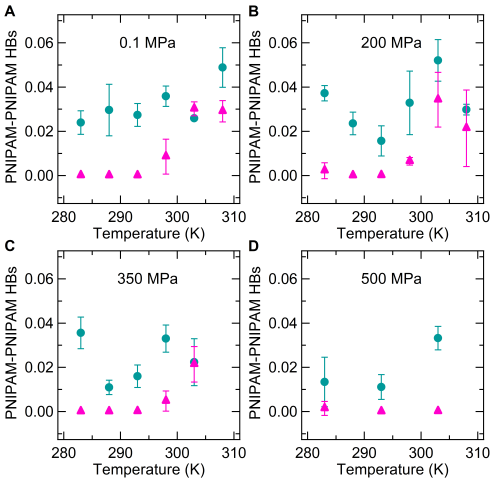

FIG. S6: Temperature dependence of the number of PNIPAM-PNIPAM hydrogen bonds between amide groups at a distance lower than 4 repeating units (blue circles) and greater than 3 repeating units (pink triangles), normalized to the number of repeating units in the chain. Data calculated at pressure values of 0.1, 200, 350 and 500 MPa are shown in panel A), B), C) and D), respectively.

VI. WATER MOLECULES STRUCTURING

To better understand the differences observed in PNIPAM hydration features, we have characterized the clustering of water molecules within the first solvation shell, defined as the number of water molecules interconnected through hydrogen bonds. Figure S7A and Figure S7B compare the changes occurring in the distribution of cluster sizes of water molecules when PNIPAM coil-to-globule transition is induced by temperature or pressure, respectively. At 283 K and 0.1 MPa we observe the presence of a large number of small clusters and a distribution of values centered at about 420 water molecules. By heating the system at 0.1 MPa a clear reduction of the average size of the distribution is observed when PNIPAM undergoes the coil-to globule transition. Differently, when pressure is increased at 283 K no such net variation is detected, which denotes a stability of the structure of the hydration shell, although the coil-to-globule transition occurs above 350 MPa. Therefore Figure S7 shows that P-induced globule states are characterized by a more structured hydration shell as compared to T-induced globule states. To probe the local order of water molecules, we have also calculated the tetrahedrality order parameter for bulk and hydration water as a function of temperature for P= 0.1, 200, 350 and 500 MPa, as shown in Figure S8. We observe that hydration water exhibits a lower tetrahedrality order parameter than in the bulk of solution. Moreover, a temperature increase monotonically reduces the structuring of both bulk and hydration water. Instead, by applying pressure the tetrahedral order of water molecules decreases in the bulk and raises in the first solvation shell.

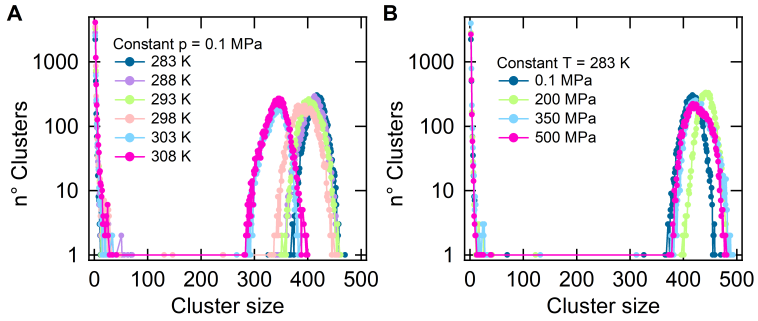

FIG. S7: Distribution of cluster sizes of water molecules in the first solvation shell of the polymer chain: A) isobaric behavior at P= 0.1 MPa and B) isothermal behavior at T=283 K. Data obtained at 0.1 MPa and 283 K, 288 K, 293 K, 298 K, 303 K, and 308 K are shown in blue, violet, green, orange, light blue and pink, respectively. Data referring to replica 1 are calculated at 283 K and 0.1 MPa, 200 MPa, 350 MPa, and 500 MPa and are displayed in blue, green, light blue, and pink, respectively.

VII. PNIPAM-WATER HYDROGEN BONDING INTERACTIONS

We investigated the changes in PNIPAM hydration properties through the characteristic lifetime of PNIPAM-water hydrogen bonding interactions, as reported in Table S1. We find a reduction of the lifetime by applying pressure, while the transition to globular conformation slightly increases it. These results are coherent with the increased mobility of PNIPAM hydration water moving from 0.1 to 130 MPa, as well as the reduction of mobility after the phase separation, as experimentally detected [S21].

TABLE S1: Lifetime of PNIPAM-water hydrogen bonds.

T (K)	0.1 MPa	200 MPa	350 MPa	500 MPa
283	126 (±8)	94 (±10)	87 (±10)	102 (±11)*
288	74 (±6)	67 (±5)	65 (±8)	
293	65 (±3)	66 (±11)	66 (±4)*	84 (±13)*
298	50 (±4)	69 (±6)*	64 (±11)*	
303	63 (±5)*	50 (±5)*	48 (±6)*	44 (±5)*
308	41 (±4)*	41 (±9)*		

Lifetimes are reported in ps. Errors are estimated by applying the blocking method. Lifetimes associated to globular conformations are marked with an asterisk. Data refer to Replica 1.

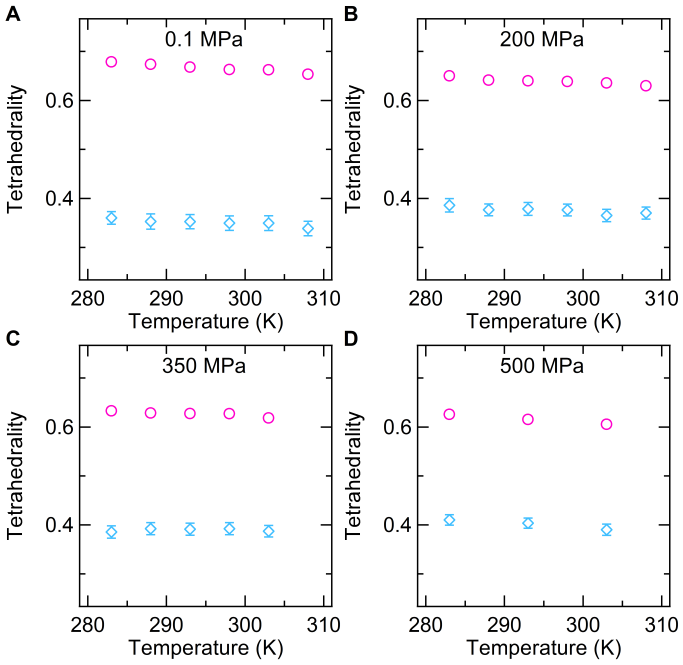

FIG. S8: Temperature dependence of the tetrahedrality order parameter calculated for hydration (blue diamonds) and bulk (pink circles) water molecules. Data calculated at pressure values of 0.1, 200, 350 and 500 MPa are shown in panel A), B), C) and D), respectively.

VIII. COMPARISON BETWEEN TWO REPLICAS AT PRESSURES BELOW 200 MPA

To verify the occurrence of the pressure reentrance we have carried out two independent replicas of the simulations at pressures below 200 MPa starting from a different initial chain conformation for the three representative temperatures (T=283, 303 and 308 K) discussed in Fig. 3 of the main text. Comparative results for the first replica versus the average of the two are reported in Figs. S9 and S10 confirming the occurrence of a reentrant behavior at low pressure.

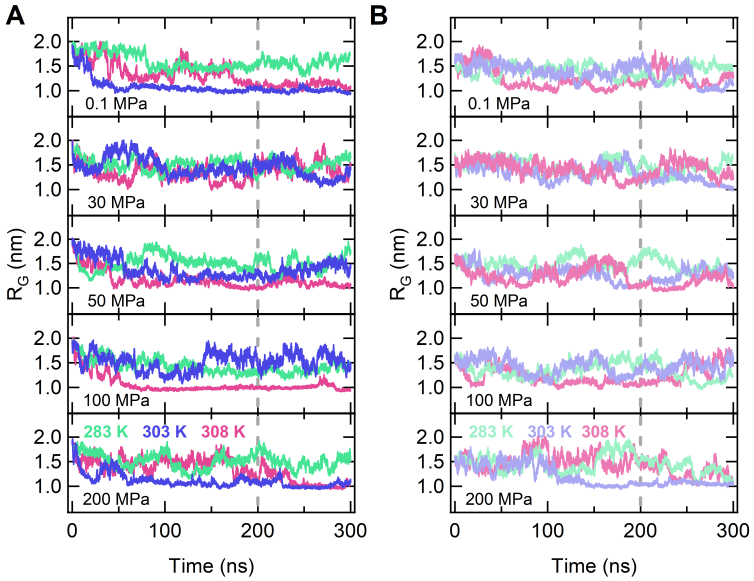

FIG. S9: Radius of gyration as a function of time for P=0.1, 30, 50, 100 and 200 MPa for A) replica 1 and B) replica 2. Data refer to T=283 K (green), T=303 K (blue), and 308 K (red).

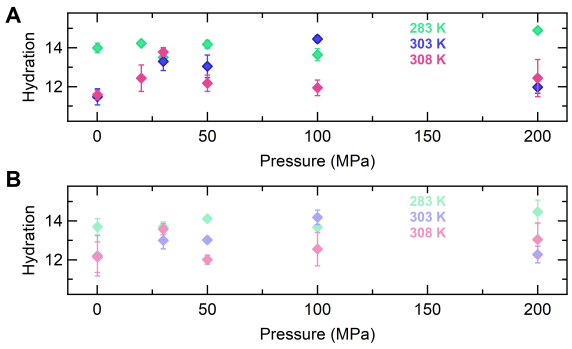

FIG. S10: Number of hydration water molecules *per* PNIPAM residue as a function of pressure for A) replica 1 and B) average between the two replicas. Data refer to T=283 K (green), 303 K (blue) and 308 K (red).

[S1] J.-F. Lutz, Ö. Akdemir, A. Hoth, Point by point comparison of two thermosensitive polymers exhibiting a similar lcst: is the age of poly(nipam) over?, Journal of the American Chemical Society 128 (40) (2006) 13046–13047.

[S2] J. Shan, Y. Zhao, N. Granqvist, H. Tenhu, Thermoresponsive properties of n-isopropylacrylamide oligomer brushes grafted to gold nanoparticles: effects of molar mass and gold core size, Macromolecules 42 (7) (2009) 2696–2701.

[S3] E. Chiessi, G. Paradossi, Influence of tacticity on hydrophobicity of poly(n-isopropylacrylamide): a single chain molecular dynamics simulation study, The Journal of Physical Chemistry B 120 (15) (2016) 3765–3776.

[S4] L. Tavagnacco, E. Zaccarelli, E. Chiessi, On the molecular origin of the cooperative coil-to-globule transition of poly (n-isopropylacrylamide) in water, Physical Chemistry Chemical Physics 20 (15) (2018) 9997–10010.

[S5] W. L. Jorgensen, D. S. Maxwell, J. Tirado-Rives, Development and testing of the opls all-atom force field on conformational energetics and properties of organic liquids, Journal of the American Chemical Society 118 (45) (1996) 11225–11236.

[S6] S. W. Siu, K. Pluhackova, R. A. Böckmann, Optimization of the opls-aa force field for long hydrocarbons, Journal of Chemical Theory and Computation 8 (4) (2012) 1459–1470.

[S7] Abascal, J. L. F.; Sanz, E.; Fernández, R. G.; Vega, C. A potential model for the study of ices and amorphous water: TIP4P/Ice, Journal of Chemical Physics 122 (2005) 234511.

[S8] Flory, P. J.; Mark, J. E.; Abe, A. Random-Coil Configurations of Vinyl Polymer Chains. The Influence of Stereoregularity on the Average Dimensions, Journal of the American Chemical Society, 88 (4) (1966) 639–650.

[S9] S. Markidis, E. Laure, Solving software challenges for exascale: International conference on exascale applications and software, easc 2014 stockholm, sweden, april 2–3, 2014 revised selected papers, Lecture Notes in Computer Science (including subseries Lecture Notes in Artificial Intelligence and Lecture Notes in Bioinformatics) 8759 (2015).

[S10] M. J. Abraham, T. Murtola, R. Schulz, S. Páll, J. C. Smith, B. Hess, E. Lindahl, Gromacs: High performance molecular simulations through multi-level parallelism from laptops to supercomputers, SoftwareX 1 (2015) 19–25.

[S11] W. Humphrey, A. Dalke, K. Schulten, Vmd: visual molecular dynamics, Journal of Molecular Graphics 14 (1) (1996) 33–38.

[S12] R. W. Hockney, The potential calculation and some applications, Methods Comput. Phys. 9 (1970) 136.

[S13] B. Hess, H. Bekker, H. J. Berendsen, J. G. Fraaije, Lincs: a linear constraint solver for molecular simulations, Journal of Computational Chemistry 18 (12) (1997) 1463–1472.

[S14] G. Bussi, D. Donadio, M. Parrinello, Canonical sampling through velocity rescaling, The Journal of Chemical Physics 126 (1) (2007) 014101.

[S15] H. J. Berendsen, J. V. Postma, W. F. van Gunsteren, A. R. H. J. DiNola, J. R. Haak, Molecular dynamics with coupling to an external bath, The Journal of chemical physics, 81 (8) (1984) 3684–3690.

[S16] U. Essmann, L. Perera, M. L. Berkowitz, T. Darden, H. Lee, L. G. Pedersen, A smooth particle mesh ewald method, The Journal of Chemical Physics 103 (19) (1995) 8577–8593.

[S17] T. J. Richmond, Solvent accessible surface area and excluded volume in proteins: Analytical equations for overlapping spheres and implications for the hydrophobic effect, Journal of Molecular Biology 178 (1) (1984) 63–89.

[S18] A. Bondi, van der waals volumes and radii, The Journal of Physical Chemistry 68 (3) (1964) 441–451.

[S19] F. Eisenhaber, P. Lijnzaad, P. Argos, C. Sander, M. Scharf, The double cubic lattice method: efficient approaches to numerical integration of surface area and volume and to dot surface contouring of molecular assemblies, Journal of Computational Chemistry 16 (3) (1995) 273–284.

[S20] J.R. Errington, P.G. Debenedetti, Relationship between structural order and the anomalies of liquid water, Nature 409 (6818) (2001) 318–321.

[S21] B. J. Niebuur, W. Lohstroh, M. S. Appavou, A. Schulte, C. M. Papadakis, Water dynamics in a concentrated poly (N-isopropylacrylamide) solution at variable pressure, Macromolecules 52 (5) (2019) 1942–1954.